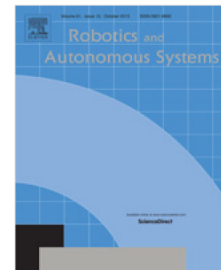# Accepted Manuscript

Active sensorimotor control for tactile exploration

Uriel Martinez-Hernandez, Tony J. Dodd, Mat Evans, Tony J. Prescott, Nathan F. Lepora

Please cite this article as: U. Martinez-Hernandez, et al., Active sensorimotor control for tactile exploration, *Robotics and Autonomous Systems* (2016), http://dx.doi.org/10.1016/j.robot.2016.09.014

Active sensorimotor control for tactile exploration

Uriel Martinez-Hernandez[a,b,*], Tony J. Dodd[a,b], Mat Evans[b], Tony J. Prescott[b], Nathan F. Lepora[c,d]

[a]Department of Automatic Control and Systems Engineering, The University of Sheffield, Sheffield, UK
[b]Sheffield Robotics Lab, The University of Sheffield, Sheffield, UK
[c]Department of Engineering Mathematics, The University of Bristol, Bristol, UK
[d]Bristol Robotics Lab, The University of Bristol, Bristol, UK

Abstract

In this paper, we present a novel and robust Bayesian approach for autonomous active exploration of unknown objects using tactile perception and sensorimotor control. Despite recent advances in tactile sensing, robust active exploration remains a challenging problem, which is a major hurdle to the practical deployment of tactile sensors in robots. Our proposed approach is based on a Bayesian perception method that actively controls the sensor with local small repositioning movements to reduce perception uncertainty, followed by explorative movements based on the outcome of each perceptual decision making step. Two sensorimotor control strategies are proposed for improving the accuracy and speed of the active exploration that weight the evidence from previous exploratory steps through either a weighted prior or weighted posterior. The methods are validated both off-line and in real-time on a contour following exploratory procedure. Results clearly demonstrate improvements in both accuracy and exploration time when using the proposed active methods compared to passive perception. Our work demonstrates that active perception has the potential to enable robots to perform robust autonomous tactile exploration in natural environments.

Keywords: Active tactile sensing, Bayesian perception, sensorimotor control, tactile exploration

1. Introduction

Humans purposefully move their hands and fingers to enhance the perceptual characteristics of objects being touched, which is known as active exploration [1, 2, 3]. Different exploratory procedures (EPs) are performed according to the type of information that is desired – for instance, pressure, contour following and sliding are used for extracting hardness, shape and texture [4, 5]. Motivated by this, recent advances in tactile sensing technology have improved the capability of robots to interact with their surrounding environment. In particular, robots equipped with biomimetic fingertip sensors are able to detect, explore and manipulate objects [6, 7]. However, despite these advances in tactile sensing technology, robust computational methods for real-time active control of biomimetic sensors during an autonomous exploratory procedure have not been developed.

This paper presents a novel and robust Bayesian approach for actively controlling a biomimetic fingertip during autonomous exploration of an unknown object. We consider a task of actively exploring object contours with two types of movement: 1) local repositioning to improve perception (fingertip position normal to contour), and 2) movements to accomplish the exploration task (edge orientation to move tangentially along the contour). We utilise a computational method for estimation of position and edge orientation based on Bayesian optimal decision making that reduces the uncertainty of the measurements from the tactile sensor. This method improves tactile perception by accumulating

---

*Corresponding author

evidence from the object being touched while moving the sensor to a good location for perception [8, 9, 10, 11]. Here we have designed this active perception method to achieve real-time control during the discrimination of a very large dataset of perceptual classes with a tactile robot. The theoretical novelty of the proposed method is that a successful autonomous exploration strategy emerges from a relatively simple sensor-centric control.

In this work we define two types of sensorimotor control strategy motivated by how human decision making can be affected by prior knowledge and current expectations, according to the weight and reliability of each source of information [12, 13]. Inspired by this, we extend our methods for active exploration investigated in [14] with two sensorimotor control strategies that combine current sensory information with prior or predicted information to analyse their benefits on the exploration performance. The first sensorimotor control strategy called 'weighted prior strategy' takes the prior as the posterior from the previous exploration step combined with a flat prior; the second sensorimotor control strategy called 'weighted posterior strategy' combines instead the posterior during active perception with predicted observations. Accordingly, a forward model is developed to predict the observations by modifying the likelihoods from the active perception method. The benefits of these sensorimotor control strategies are observed in improvements to both the accuracy and speed of exploration.

To validate our autonomous active exploration methods, we choose a contour following exploratory procedure inspired by how humans use touch to extract the shape of an unknown object. Our methods are first validated in a simulated environment using real data from a tactile fingertip, and then secondly in a real environment on a Cartesian robot to extract various shapes in real-time. These simulated and real-time validations demonstrate the benefits of active over passive perception to successfully accomplish an autonomous exploration task using tactile sensing. Furthermore, the implementation of the proposed sensorimotor control strategies indicates how the weight and reliability of the information improve the perceptual accuracy and speed during the exploration task. The findings of this investigation provide new robust and accurate computational methods to exploit the advances and integration of tactile sensing technology in robotics.

The remainder of this article is organised in four sections. First, a literature review on tactile data processing, edge detection and tracking is presented. Second, the equipment, data collection and methods used for this study are described. Next, the results from simulations and robotic experiments are presented. Finally, the article provides a discussion of the findings, limitations and future research.

2. Related work

Artificial tactile sensors have been utilised in robots for many decades, enabling sensorised robots to interact physically with their surrounding environment. Planar tactile sensor technology has been widely used in robotic arms, hands and grippers. The geometry of this sensor technology means that measurements are gathered as a data matrix, which is commonly analysed with image processing algorithms [15, 16]. However, these imaging methods are not the most appropriate for biomimetic fingertip sensors, which given their rounded shape, small size and limited number of taxels cannot be treated as tactile images. Biomimetic sensor technology inspired by human fingertips is more suitable for enabling humanoid robots to manipulate, perceive and interact with objects in their environment [17]. A detailed review on advances in technology for design and fabrication of tactile sensors, and their applications in robotics is presented in [18].

Methods for tactile perception with biomimetic fingertip sensors can be distinguished into two types, known as passive and active perception [2, 3]. In passive perception, the fingertip interacts with an object to obtain tactile data for classification, but this data cannot affect the motion of the fingertip; conversely, in active perception, a sensorimotor feedback loop controls the fingertip to move to a better location for perception during the decision making process [14, 11]. Previous work has shown that passive tactile perception can be non-robust in unstructured environments where the position of objects is initially unknown, whereas active perception with a suitable control policy is able to correct for initially poor contacts [10]. In consequence, active perception can give an order-of-magnitude improvement in perceptual acuity over passive methods [19].

In human behavioural experiments, active exploration with tactile sensing has been studied through a contour following exploratory procedure, given that this is a common exploration to extract object shape information [20, 21]. In robotics, edge detection has been investigated analysing the data from tactile images [22, 23]. These methods used image processing techniques to detect the edge and its orientation from the data array. Estimation of curvature for contour following was implemented by controlling the contact force, position and orientation of planar tactile sensors [24, 25, 26]. However, these methods did not consider uncertainty in the measurements and the control was based only on information from the current tactile contact during the exploration task. A superior control framework for tactile exploration using a planar sensor array was presented in [27]. This approach was based on geometrical moments from tactile images; however, such methods apply only to planar sensors composed of large arrays of taxels, not biomimetic tactile fingertips as discussed at the beginning of this section. Some methods based on active exploration of deformable objects, deformation of rounded fingertip sensor, sliding and rolling the sensor over an object being touched were implemented with a contour following exploration task [28, 29]. Active perception for edge detection, based on sensor palpations, was investigated and validated in simulated and in real-time experiments using a probabilistic approach and a biomimetic fingertip [9, 14].

There are several related probabilistic methods for extracting object features with tactile fingertips. The approach used here is built on an evidence accumulation framework for optimal decision making utilising tactile sensors [30, 31, 32], later extended to actively repositioning the tactile sensor during perception [8, 10, 11]. Another method for exploration of shape and extraction of local environment properties was implemented using force sensors applied to surgical robots [33]. Meanwhile, a probabilistic approach for object localisation using touch has been proposed in [34], providing good accuracy but not including active behaviour to move the sensor to better locations for perception.

A related formalism termed Bayesian exploration [35] has superficial similarities to that used here, but there are important differences in the active perception method. The approach in [35] concerns selecting explorative movements that maximally disambiguate potential perceptual hypotheses. Conversely, here we adopted a method that uses small corrective movements during active perception to approach a preset good location for decision making [14, 9, 11], which is more analogous to feedback control and therefore suited to a contour following task. Here, the feature identification is used to guide the exploration with simple fixed rule, so that the exploration emerges from the perception. For example, a simple strategy of moving perpendicularly to an edge, once the edge angle has been perceived, will lead to a contour-following exploration of that edge.

3. Methods

3.1. Biomimetic fingertip sensor

For this work, we used a biomimetic fingertip sensor that is part of the tactile sensory system of the iCub humanoid robot [36]. This tactile sensory system provides the iCub humanoid robot with capabilities to interact with its environment [37]. The tactile sensor resembles a human fingertip, given its rounded shape and dimensions (14.5 mm long by 13 mm wide; shown in Figure 1).

The tactile fingertip is built around a capacitive technology containing an array of twelve taxels (tactile elements) of ∼4 mm diameter each. These taxels cover the inner core of the fingertip with a flexible printed circuit board (PCB), with a ∼2 mm dielectric layer of silicone foam placed above the PCB. The flexible and conductive outer layer is composed of a carbon black silicone material, which also allows deformations of the surface of fingertip sensor, analogous to those that occur with the human fingertip. The capacitive measurements read from the taxels are digitised locally using a capacitance-to-digital converter (CDC) placed in the PCB above the inner core of the tactile sensor. The digital measurements from the CDC are sent to a computer through a CAN-bus to be processed. The 12 capacitance measurements obtained with a sample rate of 50 Hz are digitised with 8 bit resolution (0–255 values).

There is a resemblance between the technology used in the tactile sensor and the mechanical and sensory structure of the human fingertip that allows perception of pressure, curvature and edge orientation [38]. In particular, the taxels in the tactile sensor respond analogously to human mechanoreceptors to brief and sustained response from tactile stimuli.
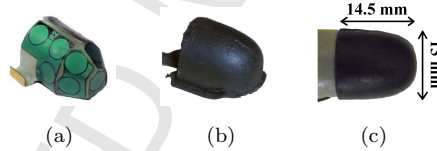

Figure 1: Biomimetic iCub fingertip sensor. (A) Arrangement of circular taxels on flexible PCB covering the inner support. (B) Outer conductive layer in a standalone fingertip. (C) Physical dimensions of the tactile sensor.

3.2. Robot

A robot was constructed to provide mobility to the fingertip sensor that is composed of two different robot components: (1) a Cartesian robot arm (YAMAHA XY-x series) with 2-DoF (degrees of freedom) in the x- and y-axes, and (2) a Mindstorms NXT Lego robot built with 1-DoF. The NXT robot is mounted on the Cartesian robot arm in a proper manner to generate movements in the x-, y- and z-axes (see Figure 2).

We mounted the tactile sensor on the robot to perform precise positioning movements in the x- and y-axes with an accuracy of ∼20 μm. The capabilities of the NXT robot do not allow very precise movements, but these are good enough to perform upwards and downwards movements along the z-axis. Robot movements in x-, y- and z- axes are controlled by tactile feedback that, based on pressure measurements from the fingertip sensor, allow to perform a tactile exploration task. Figure 2 shows the fingertip sensor mounted on the robot platform. This configuration of the robot and the degrees of freedom do not allow rotations around the z-axis of the tactile sensor. Therefore, the fingertip sensor keeps the same orientation during all experiments.
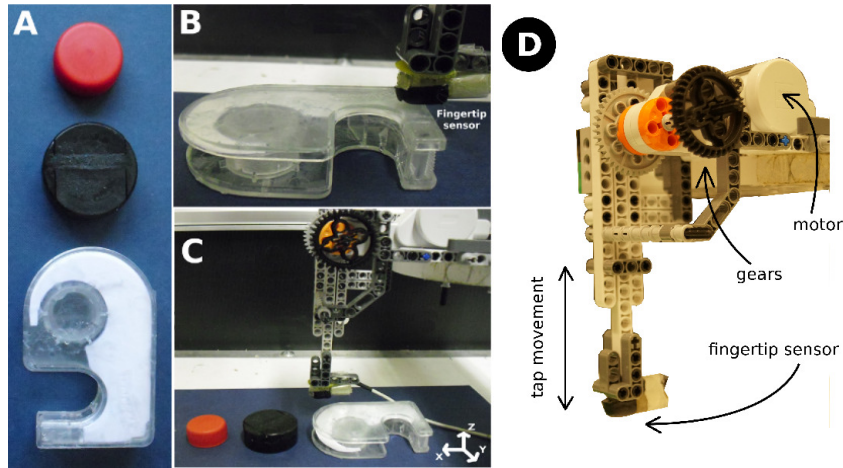
4

Figure 2: (A) Different shaped and sized objects used for active Bayesian perception applied to sensorimotor control. Two of these objects have diameters of $2\,cm$, $4\,cm$, while the third object with irregular shape has various radii of curvature. All the objects have a height of $1\,cm$. (B) Biomimetic fingertip sensor in contact with the edge of an object at one angle and position. (C) Tactile sensor mounted on a Cartesian robot allowing mobility in x-, y- and z- axes. (D) Mechanism of the NXT robot built to perform upwards and downwards movements along the z-axis with the fingertip sensor.

¹¹⁹ A tactile exploration based on taps was chosen for two main reasons. First, to reduce damage to the sensor because,
¹²⁰ in contrast, a sliding motion could deteriorate the outer conductive layer after repeating the experiments several times.
¹²¹ Second, to utilise tactile exploration movement through repetitive palpations, useful for robotic system that are not
¹²² able to slide their sensors. Even though tactile fingertips are different in form to rats' whiskers, a palpating exploratory
¹²³ procedure with a fingertip is analogous to the whisking movements that rats use to explore their environment. Humans
¹²⁴ typically slide their fingertips during exploration of shape; however, in situations where there is an expectation that
¹²⁵ damage may occur or for inspection of delicate objects (e.g. medical diagnosis), we can also perform a palpating
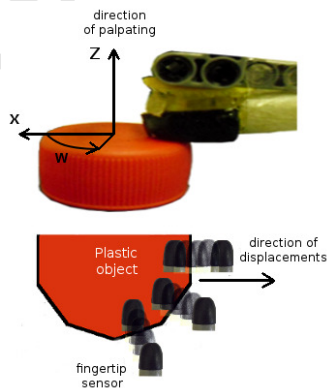¹²⁶ exploratory procedure.

Figure 3: Data collection procedure from an edge stimulus of a plastic object. The fingertip sensor collects data based on taps along the z-axis and displacement movements along x- and y-axes. The data are collected at $5\,\mathrm{deg}$ steps with taps along $18\,\mathrm{mm}$ at $0.2\,\mathrm{mm}$ steps perpendicular to the edge. For visualisation, we show only three examples of data collection with the fingertip sensor. In total we collected data from 72 angles and $18\,\mathrm{mm}$ positions each.

5

127 *3.3. Data collection*

128 We collected two distinct sets of tactile data for training and offline validation, exploring a single flat circular object
129 in a systematic and well-controlled procedure. The object was rigidly attached to the table to prevent slippage. Data
130 were collected by tapping against the object over different locations in the x-y plane sampled in polar coordinates.
131 That is, given a fixed orientation angle w the object is tapped along a line radially extending from the inside of the
132 object (with full contact), passing over the edge (with partial contact), and ending outside the object (with no contact)
133 (Figure 3). Along this line, taps were performed in 0.2 mm steps over a distance of 18 mm, generating a total of 90
134 taps for each edge orientation. The orientation angle was changed in steps of 5 deg yielding 72 direction measurements
135 for a full 360 deg coverage. A single tap had a duration of 2 sec, yielding a dataset of 12×100 pressure measurements
136 from the fingertip sensor (sampling frequency 50 Hz and 12 taxels). Figure 4 shows an example of the pressure signals
137 obtained by a single tap at full contact on the object, over the edge and outside the object.
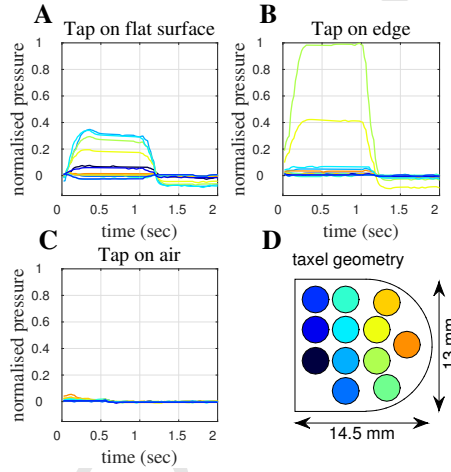

Figure 4: Tactile data at flat surface, edge and air for the fingertip sensor tapping with an angle orientation of 0 deg. (A) Tap on flat surface, where the pressure is spread to most of the taxels. (B) Tap on edge where the pressure is concentrated in a small number of taxels. (C) Tap on air, where the sensor is not in contact with the stimulus. (D) Coloured taxels layout that allows to visualise which parts of the fingertip sensor are activated for data collection at flat surface, edge and air regions.

138 Figure 5 shows examples of the normalised tactile data collected with the fingertip sensor. The pressure of the
139 taxels in contact with the object gradually changes along the trajectory of data collection. These variations in the
140 pressure are related to the orientation and positioning of the fingertip with respect to the object. Hence, from the
141 tactile data we are able to perceive both the angle and position of the fingertip sensor relative to the edge of the object.
142 Note also the present of noise — for example, the peaks just outside the object are from mechanical jerking of gears
143 in the robot.

144 We built position classes using groups of 5 taps per class, from the 90 taps performed for each edge orientation, and
145 were each group represents a position class. Then, we obtained a total of 18 position classes of 1 mm span each. These
146 were used to construct the classifier based on histograms [30] (Section 3.4), and moreover gave classes representing
147 a span of locations rather than a single position. In total, we formed a large dataset composed of 72 angles × 18
148 positions = 1296 perceptual classes. As mentioned earlier, the complete process was repeated twice to collect one
149 dataset for testing and one for training, with differences between these sets being characteristic of the accuracy and
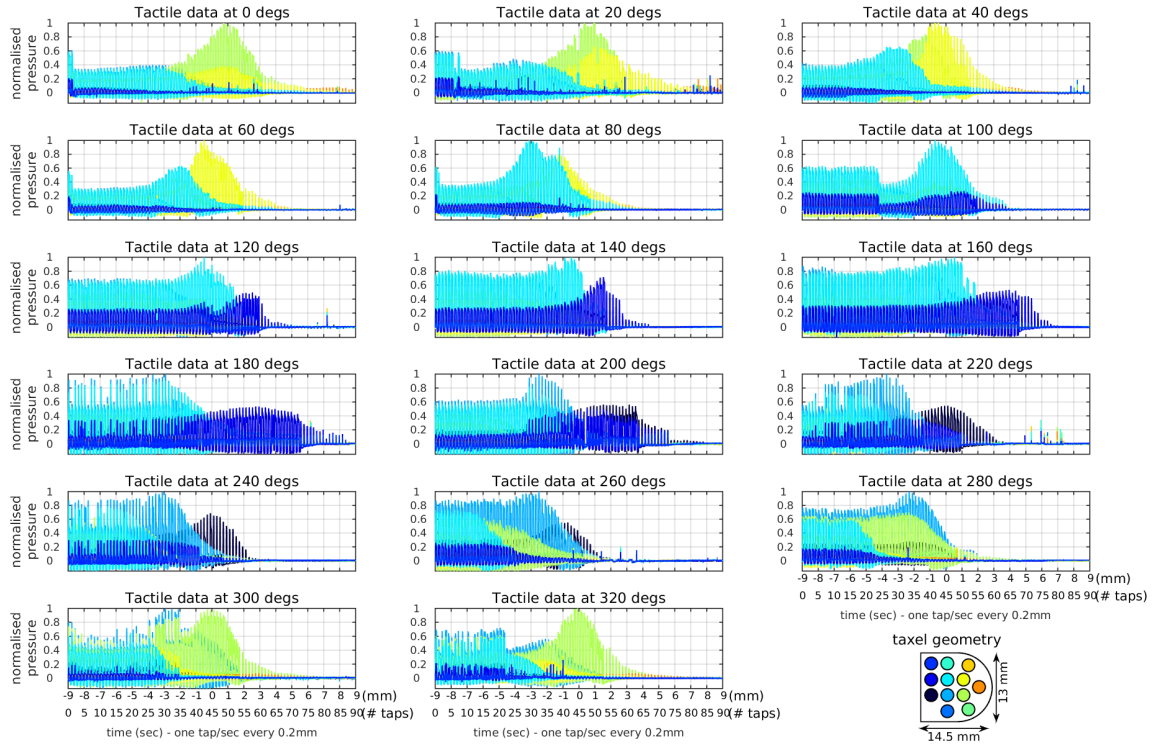150 repeatability of the robot.

6

Figure 5: Tactile data collected using the method described in Section 3.3. The data collection was at 5 deg steps around a plastic object with displacement steps of 0.2 mm perpendicular to the edge of the object. This was repeated 72 times covering the 360 deg of a circle. For each angle step, we took 90 contacts each within 2 seconds of data (100 samples per taxel) across the 18 mm range of positions, taking 72×90 = 6480 contacts. The colouring of the figures denote the distinct taxels. For visualisation, here we show only 17 figures (of the 72) with data collected every 20 deg. All data within each figure are shown, but only the envelopes of the peak taxel readings are visible because of the density of contacts displayed.

3.4. Active Bayesian perception

Perception can be considered as either active for situations where sensory data affects the control of the sensor, or passive when the sensory data does not affect the motion of the sensor relative to the stimulus [1, 2]. The ability to control sensor movements using active perception based on previous sensory data, for example to explore areas of apparent interest, gives an improvement to the perceptual performance, such as the decision speed and perceptual accuracy.

Our active exploration framework is based on methods for active Bayesian perception, which have been validated with various stimuli such as textures and shapes using the biomimetic iCub fingertip [9, 11]. These validations have shown the versatility of these methods over a range of tactile robotic applications. The methods implement Bayes' rule through a technique of sequential analysis [39], which recursively updates the posteriors with likelihoods obtained from a measurement model of the tactile data until reaching a decision threshold.

Here, we applied active exploration to follow the unknown contour of various object shapes with a tactile fingertip sensor. The sensor performs active repositioning movements to make better perceptual decisions about its location and orientation (angle) relative to edge being followed. Once a decision is made, the sensor uses this information to move along the contour, so that it may continue the exploration and thus extract the complete contour of the object. Therefore, we use active perception for two reasons: 1) to improve classification performance by moving the fingertip to good positions for angle perception; and 2) to provide feedback into a sensorimotor architecture to control movements

7

b	bin index	w_i	angle class	w_{dec}	angle decision
N_{bins}	number of bins	z_t	contact at time t	x_{loc}	position decision
N_{samples}	number of samples	$z_{1:t}$	contact history at time t	x_{fix}	target position
N_{taxels}	number of taxels	$P(c_n)$	uniform prior	π	movement policy
N_{loc}	number of position classes	$P(z_t|c_n)$	location likelihood	$P_{\text{flat}}(c_n)$	uniform prior
N_{id}	number of angle classes	$P(z_t|z_{1:t-1})$	marginal probability	$P_{\text{fwd}}(c_n|\tilde{z}_T)$	forward model
$h_{kn}(b)$	sample histogram	$P(x_l|z_{1:t})$	position belief	$P_{\text{prior}}(c_n|z_0)$	weighted prior
c_n	location class	$P(w_i|z_{1:t})$	angle belief	$P_{\text{posterior}}(c_n|z_t)$	weighted posterior
x_l	position class	θ_{dec}	belief threshold	decision time	T

Table 1: Terms and definitions

of the tactile sensor during the exploration task. Overall, the active Bayesian perception method consists of five layers, which are described in the following paragraphs.

3.4.1. Sensory layer

The first part of the algorithm is the acquisition of tactile measurements. In this process a dataset composed of 12×100 pressure measurements is collected by the fingertip sensor with sampling frequency of $50\,\text{Hz}$. The data collection is based on taps (palpations).

3.4.2. Perception layer

Active perception is implemented as an estimation of contact location and orientation, in which active control of location aids identification of edge orientation. Position is thus treated as 'location' and the angle as 'identity', so that procedure may be thought of as simultaneous localisation and identification (SOLID) [8]. The classification is over N_{loc} position classes x_l and N_{id} angle classes w_i, with a total of $N = N_{\text{loc}}N_{\text{id}}$ 'position-angle' classes $c_n = (x_l, w_i)$. The tth tactile contact is represented by z_t and $z_{1:t-1}$ the tactile contact history.

Measurement model and Likelihood estimation: From each tap (z_t) we obtain a (2 second) time series with N_{samples} = 100 samples of digitised pressure values from each of the N_{taxels} = 12 taxels. The measurement model is constructed off-line from these sensor values using a nonparametric (histogram) estimation approach commonly used for statistical hypothesis testing. The measurement model is obtained from the frequency of (binned) sensor readings in the training data for each class

$$P_k(b|c_n) = \frac{h_{kn}(b)}{\sum_{b=1}^{N_{\text{bins}}} h_{kn}(b)}, \tag{1}$$

where $h_{kn}(b)$ is the sample count in bin b for taxel k over all training data in class c_n. The histograms were uniformly constructed by binning the sensor values into $N_{\text{bins}} = 100$ intervals. Then, for a test tactile contact z, the measurement model is built from the mean log likelihood over all samples, also taking into account the contribution from all taxels,

$$\log P(z|c_n) = \sum_{k=1}^{N_{\text{taxels}}} \sum_{j=1}^{N_{\text{samples}}} \frac{\log P_k(s_k(j)|c_n)}{N_{\text{samples}}N_{\text{taxels}}}, \tag{2}$$

where $s_k(j)$ is the sample j in taxel k. The model treats all samples as independent and identically distributed for each tap and taxel. Although the independence assumption may be violated in practise, it gives a good first approximation

8

for constructing a simple likelihood model, with the caveat that results could be improved by utilising statistical dependence of the data. Technically, this measurement model becomes ill-defined if any histogram bin is empty, which is easily fixed by regularising the bin counts with a small additive constant [8].

Priors: We assume uniformly distributed priors for all perceptual classes $P(c_n) = P(c_n|z_0) = 1/N$. This defines the posteriors at time $t = 0$, which will be recursively updated with the likelihoods from each tap performed by the sensor.

Bayesian update: For updating the posterior probabilities $P(c_n|z_{1:t})$, we use a recursive implementation of Bayes' rule over all N perceptual classes c_n with the likelihoods $P(z_t|c_n)$ of the measured tap z_t. The prior takes the value of the posterior at tap $t-1$ resulting in an update,

$$P(c_n|z_{1:t}) = \frac{P(z_t|c_n)P(c_n|z_{1:t-1})}{P(z_t|z_{1:t-1})}. \tag{3}$$

In order to give properly normalised values, the marginal probabilities are conditioned on the previous tap and calculated from the sum

$$P(z_t|z_{1:t-1}) = \sum_{n=1}^{N} P(z_t|c_n)P(c_n|z_{1:t-1}). \tag{4}$$

Marginal angle and position posteriors: Each class c_n corresponds to an (x_l, w_i) pair where x_l and w_i are the position and angle for each perceptual class respectively. The posteriors are the joint distributions over these joint classes, then the beliefs over individual angle and position perceptual classes are given by the marginal posteriors

$$P(x_l|z_{1:t}) = \sum_{i=1}^{N_{\mathrm{id}}} P(x_l, w_i|z_{1:t}), \tag{5}$$

$$P(w_i|z_{1:t}) = \sum_{l=1}^{N_{\mathrm{loc}}} P(x_l, w_i|z_{1:t}), \tag{6}$$

with the position beliefs summed over all angle classes and the angle beliefs summed over all position classes.

3.5. Stop rule and decision layer

A threshold crossing rule is used to stop accumulating evidence and make a decision about the angle and position class. The *maximum a posteriori* (MAP) estimate is used to decide the angle and position perceptual class when the angle belief exceeds a threshold

$$\begin{aligned} &\text{if any } P(w_i|z_{1:t}) > \theta_{\mathrm{dec}} \\ &\text{then } w_{\mathrm{dec}} = \arg\max_{w_i} P(w_i|z_{1:t}), \end{aligned} \tag{7}$$

where w_{dec} is the angle class estimated after tap t. The estimated angle w_{dec} is employed in the contour following exploration presented in Section 4.2 to move the tactile sensor along the edge of an object. We use the angle decision threshold $\theta_{\mathrm{dec}} \in [0, 1]$ to set the trade-off between decision speed and accuracy. The use of the angle class as the stopping criterion is appropriate for our chosen task of contour following because it is the angle decision that determines the direction of the next exploration step along the contour, as presented in Sections 4.2 and 4.3.
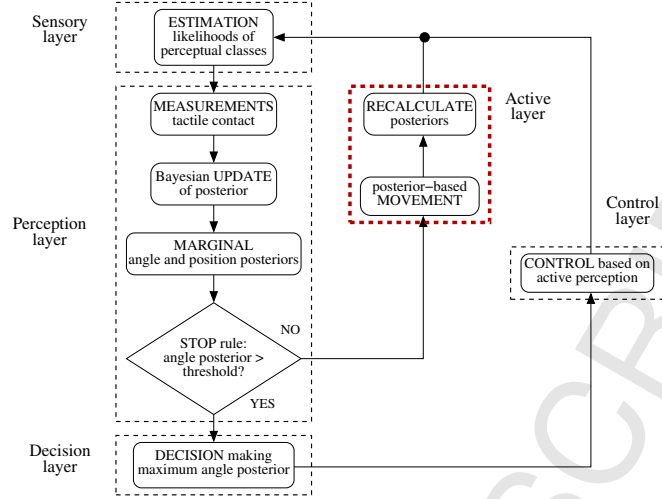
Figure 6: Active perception algorithm. The *sensory* layer reads the tactile measurements from the sensor. The *perception* layer is responsible for updating the evidence accumulated based on Bayes' rule. The decision-making based on the MAP estimate once the belief threshold is crossed is performed in the *decision* layer. The *active* layer permits to the sensor to be repositioned for improvement of perception. The output from the decision-making process is used by the *control* layer for enacting the corresponding action.

3.5.1. Active layer

In previous work, we have found that for this biomimetic fingertip sensor the perception is improved towards its centre [8, 9]. Also, as we will see later, this is supported by our results (Section 4.1). Therefore, for active perception we assume that there is a preset target position x_{fix} at the centre of the sensor that the active control seeks to attain from an initially unknown fingertip location. The movement policy represented by π is then determined from the current position estimation x_{loc},

$$x_{\mathrm{loc}} = \arg\max_{x_l} P(x_l | z_{1:t}), \tag{8}$$

$$x \leftarrow x + \pi(x_{\mathrm{loc}}), \qquad \pi(x_{\mathrm{loc}}) = x_{\mathrm{fix}} - x_{\mathrm{loc}}, \tag{9}$$

where $\pi(x_{\mathrm{loc}})$ updates the value of x which is the new position of the sensor.

The number of updated or repositioning movements performed by the sensor is related to the belief threshold. Low belief thresholds are exceeded quickly, not allowing the repositioning of the sensor to a good location for perception x_{fix} to result in fast but low accuracy decisions. Conversely, high belief thresholds require a large number of repositioning movements, because the position estimate may be incorrect, which allows a gradual repositioning of the sensor to a good location for perception to result in accurate but slow decisions. The flowchart in Figure 6 shows the sequence of steps required to perform our active perception algorithm.

3.5.2. Control layer

The decision about the location of the tactile sensor is used to calculate the next location to move the sensor along the object contour being explored. The estimated angle w_{dec} is used to calculate the next exploratory movement of the sensor in Cartesian coordinates:

$$\mathrm{MOVE} = (d\cos w_{\mathrm{dec}}, d\sin w_{\mathrm{dec}}) \tag{10}$$

10

defined by moving a fixed distance $d = 2\,\mathrm{mm}$ (Figure 7) along the perceived angle of the edge. Once the robot moves the fingertip sensor to the new position, the complete active Bayesian perception process is repeated.

The length of translation for each exploratory movement, after each angle decision, is set to a fixed value (of $2\,\mathrm{mm}$). In principle, the translation step could vary along the exploration path, but this would require forward models that are adaptive and hence go significantly beyond the present treatment.
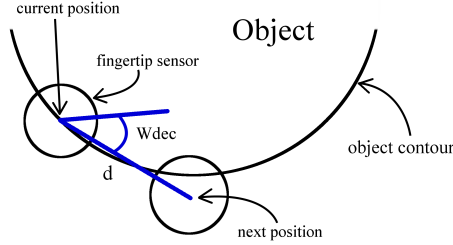

Figure 7: Calculation of the next position along the object contour based on the current position and perceived angle w_{dec}. After moving, the active perception process is repeated, ensuring that the fingertip follows the object contour.

3.6. Sensorimotor control strategies

We extend the above active perception method by combining it with two sensorimotor control strategies (Figure 8). The strategies are based on a weighted combination of present and preceding information, where the weight parameterises the reliability of each source [40]. We will examine later how these strategies affect the speed and accuracy of the exploration.

3.6.1. Weighted prior

Our first sensorimotor control strategy is called 'weighted prior strategy', and modifies the prior used in the active angle perception according to the perceptual decision from the previous exploratory step. Previous works [9, 14] have used a flat prior, which is equivalent to treating each decision as independent. However, the preceding posterior probability represents an important source of knowledge that if properly used by the forward model can improve predictions for the next angle observation.

Here we consider a prior for the current perceptual decision as a weighted combination of the preceding posterior with a uniform distribution. Denoting this preceding posterior by $P_{\mathrm{fwd}}(c_n|\tilde{z}_T)$ and the uniform distribution by $P_{\mathrm{flat}}(c_n) = 1/N$, the prior is

$$P_{\mathrm{prior}}(c_n|z_0) = \alpha P_{\mathrm{fwd}}(c_n|\tilde{z}_T) + (1 - \alpha)P_{\mathrm{flat}}(c_n), \tag{11}$$

with $\alpha \in [0, 1]$ parameterising the importance of preceding information. Thus $\alpha = 0$ corresponds to discarding preceding information, so each decision is independent; $\alpha = 1$ ensures that perceptual decisions are made only from preceding information (since the prior is always above decision threshold).

In the above, the probability distribution $P_{\mathrm{fwd}}(c_n|\tilde{z}_T)$ is taken from a forward model applied to the posteriors $P(c_n|\tilde{z}_T)$ from the *preceding* exploration step. For this study, we assume that the forward model is a $\Delta = 5\,\mathrm{deg}$ increment (one angle class) for each exploration step, compatible with the angular resolution of the training data (see Section 3.3). Hence

$$P_{\mathrm{fwd}}(c_n|\tilde{z}_T) = P_{\mathrm{fwd}}(x_l, w_i|\tilde{z}_T) = P(x_l, w_i + \Delta|\tilde{z}_T), \tag{12}$$
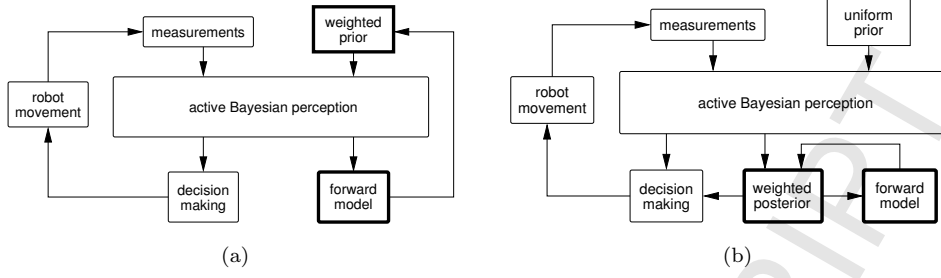
11

Figure 8: (A) Sensorimotor control based on a weighted prior. The posterior from active perception from the previous decision is used as a prior weighted by a confidence factor. This prior is also shifted by a parameter $\Delta = 5\,\mathrm{deg}$. (B) Sensorimotor control strategy based on a weighted posterior. The decision making is based on the weighted combination of the posterior from active perception and predicted observations. The updated posterior is shifted by a parameter $\Delta = 5\,\mathrm{deg}$ and used for prediction of the current decision.

where $w_i + \Delta$ are the angle observations shifted by Δ.

The movement of the tactile sensor along the contour of the object being explored is performed by the 'Control layer', which uses the estimated angle class to accomplish the exploration task. Thus, the forward model is designed to affect only angle classes w_i. Position classes x_l, which are not affected by the forward model, are still locally controlled based on active repositions (equations 8 - 9). The weighted prior strategy is shown in the diagram of Figure 8a.

3.6.2. Weighted posterior

Another approach is to combine the posterior from the preceding exploration step with the posterior from the current exploration step, to obtain a weighted posterior that can be compared with the threshold criterion for decision termination. Technically, this is equivalent to using information from the preceding exploration step to modify the decision thresholds for the perceptual choices, but is easier to implement with the posteriors.

Thus the 'weighted posterior' sensorimotor control strategy uses a posterior

$$P_{\mathrm{posterior}}(c_n|z_t) = \alpha P_{\mathrm{fwd}}(c_n|\tilde{z}_T) + (1-\alpha)P(c_n|z_t), \tag{13}$$

that combines the present posterior $P(c_n|z_t)$ at tap t with the predicted posterior $P_{\mathrm{fwd}}(c_n|\tilde{z}_T)$. (All notation is the same as the weighted prior strategy, above, including the same forward model (12).) The parameter $\alpha \in [0,1]$ again represents the importance of preceding information: $\alpha = 0$ corresponds to discarding preceding information, and $\alpha = 1$ ensures decisions are made only from preceding information.

The resulting posterior (13) then provides position $P_{\mathrm{posterior}}(x_l|z_t)$ and angle $P_{\mathrm{posterior}}(w_i|z_t)$ probabilities from analogous equations to (5) and (6). In consequence, the final angle decision for each exploration step is given by

$$\begin{aligned} &\text{if any } P_{\mathrm{posterior}}(w_i|z_t) > \theta_{\mathrm{dec}} \\ &\text{then } w_{\mathrm{dec}} = \arg\max_{w_i} P_{\mathrm{posterior}}(w_i|z_t). \end{aligned} \tag{14}$$

Note the active perception is also affected via the location estimate $x_{\mathrm{loc}} = \arg\max_{x_l} P_{\mathrm{posterior}}(x_l|z_t)$. The weighted posterior strategy is shown in the diagram of Figure 8b.

12

4. Results

4.1. Off-line validation of passive and active perception

Passive angle and position perception: First, we investigate how evidence accumulation across successive taps can lead to successful perception, with no feedback from perception into the control of the sensor. A tapping process without repositioning the sensor was repeated until the belief for one of the angle classes crossed a threshold, which then triggered a decision about the angle and position where the fingertip is located. This approach is known as passive Bayesian perception, meaning that the tactile fingertip is not able to move to another location to improve perception. The validation was based on an off-line Monte Carlo method with 10,000 iterations per belief threshold taken over the range $\theta_{dec} \in [0.0, 0.05, \ldots, 0.95, 0.99]$. For each iteration of the simulation process, data was randomly sampled with replacement from one of the 1296 (72 angle by 18 position) test classes until reaching decision threshold, using the validation and training data described in Section 3.3. This experiment was based on the flowchart in Figure 6, removing the modules in the red dashed-line box and considering only the inner loop.

Figure 9 shows the results for passive angle (top panel) and position (bottom panel) perception over 72 angle classes with the smallest mean classification error of 3.7 deg, measured as the mean absolute difference between the perceived and actual angle class averaged over simulation trials. The bottom of Figure 9 shows the number of taps required to make a decision for each belief threshold. The decision time was averaged over the number of taps required for
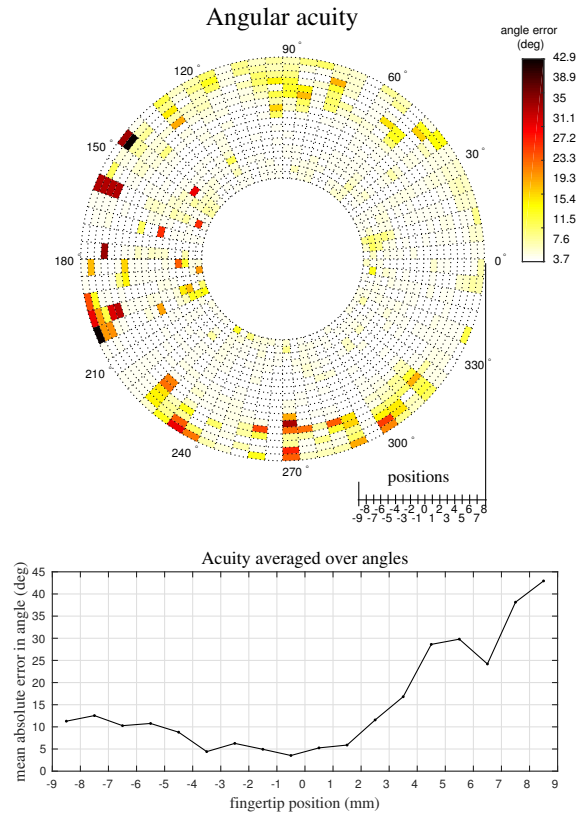

Figure 9: Angle acuity based on a passive Bayesian perception. The top 'ring' figure shows the accuracy classification over 72 angles and 18 position perceptual classes. Acuity is measured by mean absolute angle error, with large and small errors shown as red and white respectively, corresponding to values presented in the colour bar. The bottom figure shows the results for position dependency averaged over the angles.
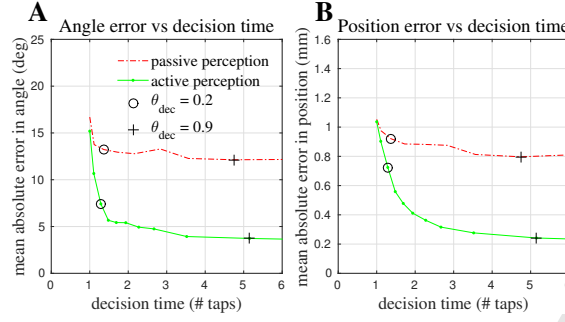
13

Figure 10: Angle and position acuity for active (green) and passive (red) perception, using an off-line Monte Carlo method. (A) Angle and (B) position errors are plotted against mean decision time. These errors are obtained by computing the mean absolute difference between the perceived and actual classes over all trials and for each belief threshold. One typical low decision threshold $\theta_{\mathrm{dec}} = 0.2$ ($\circ$) and high threshold $\theta_{\mathrm{dec}} = 0.9$ ($+$) are shown.

making a decision over the 10,000 iterations. We observe that the best position class for perception is at 0 mm, at the mid-point of the considered position range and roughly at the centre of the fingertip sensor.

Active angle and position perception: Next, we examine active perception with a sensorimotor control loop that moves the fingertip to improve perception based on tactile feedback (Figure 6). We used the training and testing datasets collected previously (see Section 3.3).

Our active perception method requires a target fixation position to move to. The results in Figure 9 indicate that the target fixation position class 0 mm provides the smallest classification error, ensuring the optimal perception. The angle and position acuity for passive perception (red curve) and active perception (green curve) plotted against mean decision time are shown in Figures 10A,B, measured by the mean absolute error averaged over all trials for each belief threshold in the range [0.0, 0.05, ..., 0.95, 0.99]. We observe the smallest angle and position errors of 12.2 deg and 0.8 mm for passive perception. In contrast, angle and position errors of 3.3 deg and 0.2 mm were obtained with active perception, showing considerable improvement over passive perception. We observe that ∼5 taps is sufficient to obtain angle and position errors close to the minimum, giving the best decisions using active perception.

4.2. Off-line validation of sensorimotor architecture

Our sensorimotor architecture is now used to implement object shape extraction in a simulated environment using the data analysed in the previous section. The implementation is composed of the modules shown in Figure 6. The simulated environment is based on a circular shaped object, corresponding to the data collected from the fingertip sensor with angle resolution of 5 deg (shown in Figure 5).

For the off-line validation we used active perception with a target position class 0 mm chosen according to the active and passive perception results from Section 4.1. The circular shaped object and the results of the autonomous active exploration with passive and active perception are shown in Figure 11. Black solid lines represent the boundaries of the exploration, whilst the contour to be traced by the fingertip sensor is shown as a black dotted line, with each dot representing an angle at 5 deg. The small green and red circles represent the locations explored by the fingertip sensor for active and passive perception. Note that in this off-line task it is not possible for the exploration to fail catastrophically, in that the sensor cannot completely lose track of the contour as it can do on the real-time task considered in Section 4.3. Instead, we quantify the quality of the contour following exploration.

Passive perception

low threshold   high threshold
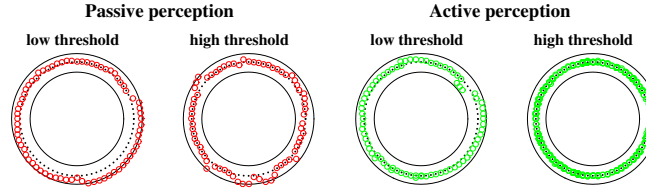
Active perception

low threshold   high threshold

Figure 11: Traced contours with active and passive exploration (off-line validation). The black dotted line represents the contour to be traced and the black solid line represent the boundaries of the exploration. The results for passive and active perception are shown for low ($\theta_{\text{dec}} = 0.2$) and high ($\theta_{\text{dec}} = 0.9$) decision thresholds. The small circles represent the locations explored by fingertip sensor. Multiple circles for high decision threshold represent the multiple taps required before making a decision. In contrast, only one tap is needed for low decision threshold.

For passive perception with low decision threshold $\theta_{\text{dec}} = 0.2$, we observe that the contour following is fast but has large angle and position errors, consistent with only small beliefs being necessary to make a decision. At high decision threshold $\theta_{\text{dec}} = 0.9$ the errors are decreased, but only slightly, even though the fingertip makes more taps on each angle decision, slowing the time to trace the contour.

For active perception with low decision threshold $\theta_{\text{dec}} = 0.2$, the fingertip sensor is actively repositioned but not able to perform enough active movements to improve perception. In contrast, active perception with high decision threshold $\theta_{\text{dec}} = 0.9$ clearly shows an improvement in angle and position perception, successfully accomplishing the contour following task. Underlying these results, if the method makes a bad initial angle and position perception (as in passive perception or active perception with low threshold), the sensor will not be able to follow the contour of the object. Conversely, for moderately inaccurate initial perception (as in active perception with high threshold), the accuracy of the angle and position perceived is corrected along the exploration, and the contours are successfully traced. Thus, our approach for active perception ensures that the exploration method will achieve good performance by correcting its perception during the task.

Summary results for passive and active exploration around the entire contour are shown in Figure 12, where the position and angle acuity is evaluated by averaging over 5000 complete loops of the contour (in contrast with Figure 10, where perceptual decisions are considered independently of contour following). For each contour, the initial location (angle and position) were randomly drawn to prevent biasing. The belief thresholds used for this validation were set to the range [0.0, 0.05, . . . , 0.95, 0.99]. Position and angle acuity is again measured by the mean absolute errors between their perceived and actual values, and displayed per decision around the contour. Evidently, the mean angle and position errors for active (green curves) perception are much improved over those for passive (red curves) perception, consistent with the qualitative observations from Figure 11 for a single contour. We observe that the smallest angle and position errors for active perception are ∼4 deg and ∼0.2 mm, averaged over a contour, which are considerably improved over the values ∼27 deg and ∼6 mm for passive perception.

Active perception and weighted prior: We analysed the effects of a weighted prior applied to active perception with the contour following task described in the previous section. The algorithmic implementation is based on the diagram shown in Figure 8a and equations (11) and (12) for weighting and shifting the prior knowledge obtained from our active perception method. The weighting α of preceding information is considered over values [0.0, 0.05, . . . , 0.95, 0.99]. Results are obtained by averaging over the individual decisions comprising the exploration around a contour for each weighting value. Again, the belief thresholds were taken over the range [0.0, 0.05, . . . , 0.95, 0.99], averaging
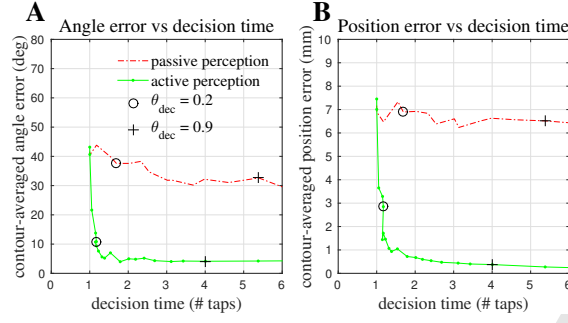
15

Figure 12: Contour-averaged angle and position acuity while performing a simulated contour following task using a circle shape constructed with real data. (A) Angle and (B) position errors for passive (red curves) and active (green curves) perception are plotted against mean decision time. All results are averaged over 5000 contour exploration loops, contrasting with Figure 10 where results are over individual decisions. One typical low decision threshold $\theta_{\text{dec}} = 0.2$ (○) and high threshold $\theta_{\text{dec}} = 0.9$ (+) are shown

337 results over 5000 contours with randomly chosen initial conditions.

338 Results are considered over the range of the prior weighting $\alpha \in [0, 1]$ (Figure 13). For $\alpha = 0$ (lightest curve),
339 the control strategy corresponds to the flat prior case considered earlier, and accordingly is identical to the results
340 in the previous section (Figure 12). For $\alpha = 1$ (darkest curve), the prior corresponds to the complete posterior from
341 the preceding time step, thereby crossing the threshold at time zero after every step of the exploration after the first
342 decision, and not being able to use new data after the first decision.

343 Overall, the speed and accuracy for angle and position exploration do not depend greatly on values of $\alpha \neq 0$, with
344 a slight performance improvement in changing from zero (flat prior) to non-zero values of α. Curiously, there is a
345 minimum in the error-decision time curve for angle perception (Figure 13A), rather than monotonically decreasing as
346 is usually the case; we interpret this as a simulation artefact due to having an exactly known forward model, so that
347 quick estimates will maintain good decisions. The smallest angle and position errors are 2.6 deg and 0.15 mm for a
348 decision time just above 1 tap and weighting α anywhere from 0.1-1. These results are improved over the performance
349 ∼4 deg and ∼0.2mm when information from preceding decisions is not used.

350 *Active perception and weighted posterior:* The application of a weighted posterior to active perception is now exam-
351 ined with the contour following task used in the previous section on the weighted prior strategy. The implementation
352 is based on the diagram shown in Figure 8b and equations (13 - 14); all other aspects of the analysis are unchanged
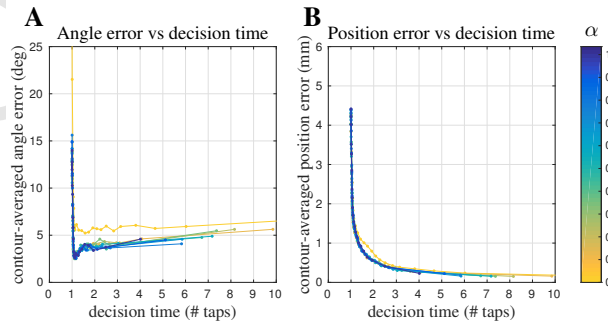353 from those above.

Figure 13: Contour-averaged angle and position acuity using sensorimotor active control with a weighted prior strategy. Mean absolute angle (A) and position (B) errors are plotted against decision time, with the weighting of the prior (α) denoted by a colour in the heat-map range from [0, 1]. Note that the results in Figure 12C,D correspond to the $\alpha = 0$ (flat prior) case here.
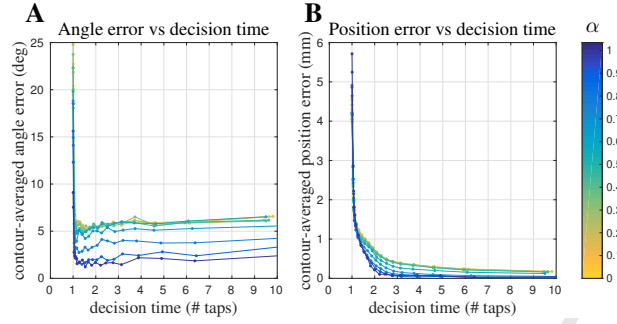
16

Figure 14: Contour-averaged angle and position acuity using sensorimotor active control with a weighted posterior strategy. Mean absolute angle (A) and position (B) errors are plotted against decision time, with the weighting of the posterior (α) denoted by a colour in the heat-map range from $[0, 1]$. The speed and accuracy of angle and position perception is improved as alpha increases until just less than 1.

Results are considered over the range of the posterior weighting $\alpha \in [0, 1]$ (Figure 14). For $\alpha = 0$ (lightest curve), the control strategy corresponds to the flat prior case considered earlier (Figure 12). For $\alpha = 1$ (darkest curve), the strategy corresponds to using the posterior from the preceding decision, which thus crosses the threshold on the initial contact. Figures 14A,B show an improvement in angle and position perception as the weighting increases for $\alpha > 0$, but then deteriorates again as α reaches 1. Both the speed and accuracy not only show a clear dependency on α but also an improvement over the original strategy considered earlier ($\alpha = 0$). The smallest angle and position errors are 1.4 deg and 0.04 mm at a reaction time of 2-3 taps for a weighting α just below 1. These results are improved over those of the weighted prior strategy and the original perception process when information from preceding decisions is not used.

For sub-optimal values of the weighting α, the results are more varied between the two control strategies, with the weighted prior strategy sometimes better than the weighted posterior strategy depending on α and the decision time. Meanwhile, for the best value of α (just below unity), the weighted posterior strategy shows a superior performance in speed and accuracy over the weighted prior strategy, and overall is the best sensorimotor control strategy.

4.3. Real-world validation

Sensorimotor architecture and active perception: We implemented a real-time contour following around a circular shaped object using our method for autonomous exploration (see Sec. 3.2 for details of the robot). In this task, the fingertip sensor performs one tap, evaluating if the belief for the current location exceeds the belief threshold. If the belief threshold is exceeded, then a decision is made, allowing the fingertip to move along the edge of the object to continue with the exploration task. If more evidence is required to make a decision, the tactile sensor is actively moved to a better position for perception, accumulating evidence until the belief threshold is exceeded.
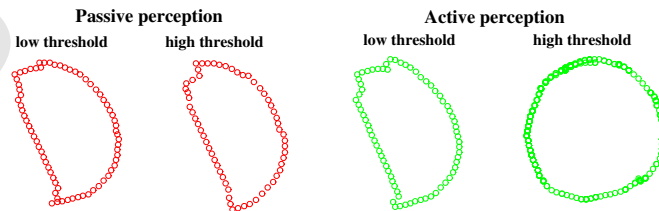

Figure 15: Traced contours of a circular object with active and passive exploration (real-time validation). Passive perception with low ($\theta_{\text{dec}} = 0.2$) and high thresholds ($\theta_{\text{dec}} = 0.9$) did not accomplished the exploration task. This behaviour was similar for active perception with low threshold. Conversely, active perception with high threshold was able to successfully trace the contour of the object.

17

We first assess whether successful contour following is achieved for either passive or active exploration with low or high decision thresholds (Figure 15). The tactile fingertip was not able to follow the contour of the object for either passive perception or active perception with a low decision threshold, since both of these cases did not permit movements to superior positions for edge classification. For active perception with high decision threshold, the fingertip sensor successfully accomplishes the contour following task, making a complete path around the object. Note that locations where active perception moved the tactile fingertip to improve angle perception are visible with multiple contacts (green circles). These are mainly visible on the left-side region of the object, and were evidently necessary for successful tracing of the complete contour.

We also validate the active exploration with various other shapes. Figure 16A shows three plastic objects used for the exploration task: two circles of 2 cm and 4 cm diameters and an irregular object (sellotape holder) with different curvatures. The height for all the objects is of 1 cm. These objects provide a good test scenario for exploration based on the wide range of angles and radii of curvature. The decision threshold $\theta_{\text{dec}} = 0.85$ is set at a high value to give a few taps per decision before making the next exploration movement. We observe in Figure 16B that the contour of the three test objects is successfully traced, which validates the robustness of our methods.
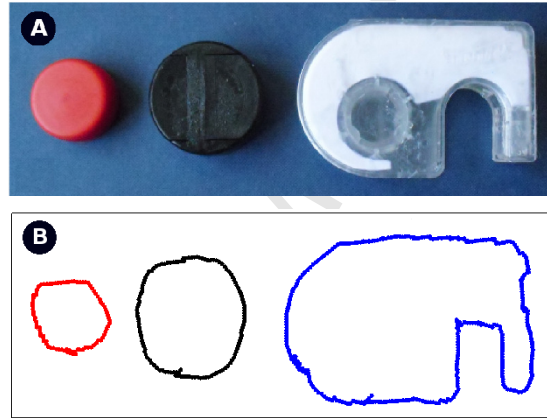

Figure 16: Contour following task using active exploration and tactile sensing. (A) Circles with 2 cm, 4 cm diameter and an asymmetric object (sellotape holder) used for real-time contour following. (B) Contours traced as result of active perception with high decision threshold.

Sensorimotor control strategies: We repeated the preceding real-time contour following procedure to validate our two proposed sensorimotor control strategies: the weighted prior and weighted posterior strategies. For these experiments, the weighting factor α between the appropriate probabilities (see Section 3.6) was set to 0.0, 0.7 and 1.0, to observe their different effects on the perception during exploration.

The results for angle and position perceptual accuracy against reaction time for both strategies are shown in Figure 17. For $\alpha = 0$, the angle and position performance is similar, as expected because the two control strategies then coincide with the unmodified case considered above. The angle performance is also worse than at non-zero α, as consistent with the off-line validation results found earlier in the paper. For $\alpha > 0$, both sensorimotor control strategies show a similar best angle accuracy with a minimum error of 1.98 deg. However, the performance of the two sensorimotor control strategies differs in the position errors, where the weighted posterior strategy has superior performance to the weighted prior strategy, and also in the reaction times where the weighted posterior strategy is apparently slower than the weighted prior strategy.

We interpret the observed change in trend of the curves in Figure 17 as related to the effects of the initial prior
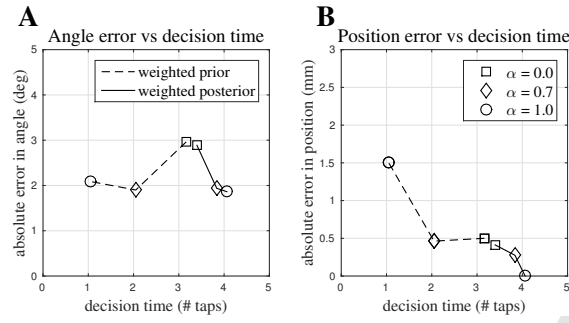
Figure 17: Comparison of weighted prior and weighted posterior strategies over a contour following task in real-time mode. The confidence factor (α) is set to values 0.0, 0.7 and 1.0 to compare their effects during the exploration task. (A) Angle and (B) position errors against decision time for the α values.

⁴⁰¹ and belief threshold on the accuracy and decision time. For the weighted prior strategy, the larger the prior the less
⁴⁰² the time required to exceed the belief threshold to make a decision; conversely, the weighted posterior strategy takes
⁴⁰³ more time to make a decision for large belief thresholds given that its initial prior is uniformly distributed. Overall, we
⁴⁰⁴ observe how the real-time exploration of an unknown object using these sensorimotor control strategies has benefited
⁴⁰⁵ by improvements in accuracy and speed, compared to the results achieved with no effect from preceding observations
⁴⁰⁶ during the exploration task.

5. Discussion

⁴⁰⁸ This study presented an investigation of autonomous active exploration using sensorimotor control of a biomimetic
⁴⁰⁹ tactile fingertip. This research demonstrated first how active movements of a tactile fingertip improve the classification
⁴¹⁰ accuracy over passive perception. Secondly, it also demonstrated how the use of sensorimotor control strategies based
⁴¹¹ on the combination of information from past and future states with active perception provide benefits for the speed
⁴¹² and accuracy of perception, hence improving the performance of the autonomous exploration of unknown objects.

⁴¹³ We found that active Bayesian perception can achieve accurate classification in edge orientation angle and po-
⁴¹⁴ sition by utilising active movements to reposition the tactile sensor to a better location for perception [9, 32]. This
⁴¹⁵ demonstrates its superiority over passive perception, where the sensor is not actively controlled. For biomimetic tactile
⁴¹⁶ fingertips, this approach makes possible edge detection with fine angular resolution, providing an alternative to image
⁴¹⁷ processing techniques [15, 16] that work only for planar sensors with high taxel densities (unlike common biomimetic
⁴¹⁸ sensors). Moreover, in principle, our method is not only applicable to edge detection but other stimuli such as texture
⁴¹⁹ and curvature [8, 10]. We validated our methods with a tactile data set of 72 angle and 18 position classes, forming a
⁴²⁰ very large set of 1296 perceptual classes. The benefits of active perception were observed in the $\sim$3.3 deg and $\sim$0.2 mm
⁴²¹ angle and position errors achieved, compared with $\sim$12.2 deg and $\sim$0.8 mm for passive perception. It is interesting
⁴²² that our results are superior in accuracy for angle discrimination to those found in both sighted and blind humans
⁴²³ under psychophysical studies using active touch [20, 21].

⁴²⁴ A new sensorimotor architecture controlled by tactile feedback was developed to provide mobility to the fingertip
⁴²⁵ sensor and validate our active perception method. During an exploration task, the tactile sensor reacts (reflex move-
⁴²⁶ ment) whenever a contact is detected to move away as a protection behaviour, and then perceive and make a decision
⁴²⁷ using active Bayesian perception, performing either a local repositioning movement for accumulating evidence or an

19

exploratory movement to next state of the exploration task. We used taps (palpations) for the exploration task for two reasons: 1) inspiration from humans in situations when they prefer to palpate rather than slide over a surface given the possibility of hurting oneself or damaging the explored object (as in medical inspection), and 2) to reduce damage to the artificial tactile sensor over multiple repetitions of the experiments.

Our tactile perception method enables a biomimetic fingertip sensor to accurately perceive edge orientation and utilise this information to perform higher level tasks, e.g. tactile exploration. This process bears analogy with studies from neuroscience that suggest that first-order tactile neurons in human fingertips are responsible for extracting geometric features (for instance, edge-orientation detection) and signal them via both temporal and rate codes [41]. Moreover, to extract object shape, humans rely on a contour following exploratory procedure using their fingers [4, 42]. This is considered an active rather than a passive exploration, meaning that the fingers need to be controlled to provide better perception.

We validated our methods for autonomous active exploration with a contour following task, and repeated this experiment with various shapes to cover a large set of angles and radii of curvature to demonstrate robustness (Figure 16). The successful shape extraction in both off-line and real-time experiments shown in Figures 11 and 15 reinforces the benefits of active over passive perception. In addition, not only is active perception necessary for task completion, but also the perception needs to be highly reliable, which is attained only for high decision thresholds. Setting a high decision threshold also increases the decision time, which slows the exploration. This is reasonable, given that humans not only explore actively but also employ the appropriate timing until sufficient belief about the object being explored is reached [43].

Finally, we investigated the effects on exploration accuracy and time of modifying the active exploration with sensorimotor control strategies that combine present sensory information with preceding or predicted information. First, we found that using a weighted prior as input to active perception produced a reduction in the angle and position errors, whilst improving the exploration time. This finding is coherent bearing in mind that less evidence would then be required to achieve faster decisions, since evidence is already present in the prior. Second, for the weighted posterior strategy, combining the output of the active perception method with predicted observations also gave improved performance accuracy and exploration. These sensorimotor control strategies show that the combination of information sources improves the performance of the autonomous active exploration. They also demonstrate that this improvement depends on the weight assigned to each information source, which corresponds to the theory of motor control in [40] and human studies of the decision making process during a discrimination task [12].

Our proposed approach for autonomous tactile exploration has been validated in two dimensions; however, we expect the methods are scalable to explore edges in three dimensions or potentially other types of path. Applying the method to more dimensions and other realistic scenarios would require a robot with more degrees of freedom, such as rotating the fingertip sensor around any axis and controlling better the height of the sensor. The systematical data collection would also need to be extended to the added degrees of freedom.

Overall, we presented a study of autonomous active exploration with sensorimotor control strategies using a biomimetic fingertip sensor. This work shows how reliability is important for tactile sensing and how this can be achieved with active perception. In robotics, this aspect of active perception can be combined with control to result in improved performance for autonomous exploration. Overall, we have demonstrated that our methods give robust autonomous tactile exploration of unknown objects, which can take advantage of the many advances taking place in

robotic sensing technology to extend to natural, complex and unstructured environments.

6. Conclusion

In this work we presented a novel and robust method, composed of active Bayesian perception and sensorimotor control strategies, for autonomous exploration of unknown object shapes using tactile sensing. Our method not only allowed a fingertip sensor to perceive and make decisions about where to move next to reduce uncertainty, but also it permitted to improve the accuracy and speed of an exploration task. Our method was validated in off-line and real-time modes, successfully exploring and extracting the contours of various object shapes. Undoubtedly, development of robust tactile perception methods, like the one presented in this work, are essential to achieve intelligent and autonomous robots that safely interact, make decisions and behave accordingly to what they perceive from its surrounding environment.

7. Acknowledgement

[1] R. Bajcsy, Active perception, Proceedings of the IEEE 76 (8) (1988) 966–1005. `doi:10.1109/5.5968`.

[2] T. J. Prescott, M. E. Diamond, A. M. Wing, Active touch sensing, Phil. Trans. R. Soc. B 366 (2011) 2989–2995. `doi:10.1098/rstb.2011.0167`.

[3] N. Lepora, Active tactile perception, in: Scholarpedia of Touch, Atlantis Press, 2016, pp. 151–159.

[4] S. J. Lederman, R. L. Klatzky, Hand movements: A window into haptic object recognition, Cognitive Psychology 19 (19) (1987) 342–368.

[5] S. Lederman, R. Klatzky, Haptic perception: A tutorial, Attention, Perception, and Psychophysics 71 (2009) 1439–1459, 10.3758/APP.71.7.1439.

[6] R. Dahiya, G. Metta, M. Valle, G. Sandini, Tactile sensing – from humans to humanoids, Robotics, IEEE Transactions on 26 (1) (2010) 1–20. `doi:10.1109/TRO.2009.2033627`.

[7] J. Tegin, J. Wikander, Tactile sensing in intelligent robotic manipulation–a review, Industrial Robot: An International Journal 32 (1) (2005) 64–70.

[8] N. Lepora, U. Martinez-Hernandez, T. Prescott, Active Bayesian perception for simultaneous object localization and identification, in: Robotics: Science and Systems, 2013.

[9] U. Martinez-Hernandez, T. Dodd, L. Natale, G. Metta, T. Prescott, N. Lepora, Active contour following to explore object shape with robot touch, in: World Haptics Conference (WHC), 2013, 2013, pp. 341–346. `doi: 10.1109/WHC.2013.6548432`.

[10] N. Lepora, U. Martinez-Hernandez, T. Prescott, Active touch for robust perception under position uncertainty, in: Robotics and Automation (ICRA), 2013 IEEE International Conference on, 2013, pp. 3005–3010.

[11] N. Lepora, U. Martinez-Hernandez, M. Evans, L. Natale, G. Metta, T. J. Prescott, Tactile superresolution and biomimetic hyperacuity, IEEE Trans. Robot 31 (3) (2015) 605–618.

[12] K. A. Hansen, S. F. Hillenbrand, L. G. Ungerleider, Effects of prior knowledge on decisions made under perceptual vs. categorical uncertainty, Frontiers in neuroscience 6.

[13] T. D. Hanks, M. E. Mazurek, R. Kiani, E. Hopp, M. N. Shadlen, Elapsed decision time affects the weighting of prior probability in a perceptual decision task, The Journal of Neuroscience 31 (17) (2011) 6339–6352.

[14] U. Martinez-Hernandez, T. Dodd, T. Prescott, N. Lepora, Active Bayesian perception for angle and position discrimination with a biomimetic fingertip, in: (IROS), 2013 IEEE International Conference on, 2013, pp. 5968–5973.

[15] A. Schneider, J. Sturm, C. Stachniss, M. Reisert, H. Burkhardt, W. Burgard, Object identification with tactile sensors using bag-of-features, in: Intelligent Robots and Systems, 2009. IROS 2009. IEEE/RSJ International Conference on, IEEE, 2009, pp. 243–248.

[16] S. Chitta, J. Sturm, M. Piccoli, W. Burgard, Tactile sensing for mobile manipulation, Robotics, IEEE Transactions on 27 (3) (2011) 558–568.

[17] P. Dario, G. Buttazzo, An anthropomorphic robot finger for investigating artificial tactile perception, The International journal of robotics research 6 (3) (1987) 25–48.

[18] U. Martinez-Hernandez, Tactile sensors, in: Scholarpedia of Touch, Springer, 2016, pp. 783–796.

[19] U. Martinez-Hernandez, N. F. Lepora, T. J. Prescott, Active haptic shape recognition by intrinsic motivation with a robot hand, in: World Haptics Conference (WHC), 2015 IEEE, IEEE, 2015, pp. 299–304.

[20] J. Voisin, Y. Lamarre, C. E. Chapman, Haptic discrimination of object shape in humans: contribution of cutaneous and proprioceptive inputs, Experimental Brain Research 145 (2) (2002) 251–260.

[21] F. Alary, R. Goldstein, M. Duquette, C. E. Chapman, P. Voss, F. Lepore, Tactile acuity in the blind: a psychophysical study using a two-dimensional angle discrimination task, Experimental Brain Research 187 (4) (2008) 587–594.

[22] N. Chen, R. Rink, H. Zhang, Efficient edge detection from tactile data, Proceedings of the 1995 IEEERSJ (1995) 386–391.

[23] A. Berger, P. Khoslar, Edge dectection for tactile sensing, in: In Proc. NASA conf. on space telerobotics, 1989, pp. 163–172.

[24] A. D. Berger, P. K. Khosla, Using tactile data for real-time feedback, The International journal of robotics research 10 (2) (1991) 88–102.

[25] N. N. Chen, H. Zhang, R. E. Rink, Edge tracking using tactile servo, Vol. 2, IEEE Comput. Soc. Press, 1995, pp. 84–89.

[26] Y. B. Kim, G. Kang, G. K. Yee, A. Kim, W. S. You, Y. H. Lee, F. Liu, H. Moon, J. C. Koo, H. R. Choi, Exploration and reconstruction of unknown object by active touch of robot hand, Intelligent Service Robotics 8 (3) (2015) 141–149.

[27] Q. Li, C. Schürmann, R. Haschke, H. Ritter, A control framework for tactile servoing, in: Proc. Robotics: Science and Systems, 2013.

[28] A. M. Okamura, M. R. Cutkosky, Feature detection for haptic exploration with robotic fingers, The International Journal of Robotics Research 20 (12) (2001) 925–938.

[29] C. Strub, F. Worgotter, H. Ritter, Y. Sandamirskaya, Using haptics to extract object shape from rotational manipulations, in: Intelligent Robots and Systems (IROS 2014), 2014 IEEE/RSJ International Conference on, IEEE, 2014, pp. 2179–2186.

[30] N. Lepora, C. Fox, M. Evans, M. Diamond, K. Gurney, T. Prescott, Optimal decision-making in mammals: Insights from a robot study of rodent texture discrimination, Journal of The Royal Society Interface 9 (72) (2012) 1517–1528.

[31] N. Lepora, M. Evans, C. Fox, M. Diamond, K. Gurney, T. Prescott, Naive Bayes texture classification applied to whisker data from a moving robot, in: Neural Networks (IJCNN), The 2010 International Joint Conference on, 2010, pp. 1–8. `doi:10.1109/IJCNN.2010.5596360`.

[32] N. Lepora, U. Martinez-Hernandez, H. Barron-Gonzalez, M. Evans, G. Metta, T. Prescott, Embodied hyperacuity from Bayesian perception: Shape and position discrimination with an icub fingertip sensor, in: Intelligent Robots and Systems (IROS), 2012 IEEE/RSJ International Conference on, 2012, pp. 4638–4643. `doi:10.1109/IROS.2012.6385649`.

[33] R. E. Goldman, A. Bajo, N. Simaan, Algorithms for autonomous exploration and estimation in compliant environments, Robotica 31 (01) (2013) 71–87.

[34] A. Petrovskaya, O. Khatib, Global localization of objects via touch, Robotics, IEEE Transactions on 27 (3) (2011) 569–585.

[35] J. A. Fishel, G. E. Loeb, Bayesian exploration for intelligent identification of textures, Frontiers in Neurorobotics 6.

[36] A. Schmitz, P. Maiolino, M. Maggiali, L. Natale, G. Cannata, G. Metta, Methods and technologies for the implementation of large-scale robot tactile sensors, Robotics, IEEE Transactions on 27 (3) (2011) 389 –400. `doi:10.1109/TRO.2011.2132930`.

[37] G. Metta, G. Sandini, D. Vernon, L. Natale, F. Nori, The icub humanoid robot: an open platform for research in embodied cognition, in: Proceedings of the 8th Workshop on Performance Metrics for Intelligent Systems, PerMIS '08, ACM, New York, NY, USA, 2008, pp. 50–56.

[38] J. Dargahi, S. Najarian, Human tactile perception as a standard for artificial tactile sensinga review, The International Journal of Medical Robotics and Computer Assisted Surgery 1 (1) (2004) 23–35.

[39] A. Wald, Sequential analysis, Courier Corporation, 1973.

[40] R. Shadmehr, M. A. Smith, J. W. Krakauer, Error correction, sensory prediction, and adaptation in motor control, Annual review of neuroscience 33 (2010) 89–108.

[41] J. A. Pruszynski, R. S. Johansson, Edge-orientation processing in first-order tactile neurons, Nature neuroscience.

[42] S. Lederman, R. Klatzky, Extracting object properties through haptic exploration, Acta Psychologica 84 (1) (1993) 29 – 40. `doi:http://dx.doi.org/10.1016/0001-6918(93)90070-8`.

[43] K. Overvliet, J. B. Smeets, E. Brenner, The use of proprioception and tactile information in haptic search, Acta psychologica 129 (1) (2008) 83–90.

Uriel Martinez-Hernandez received the BEng degree in Communications and Electronics from the National Polytechnic Institute, Mexico City, Mexico, in 2005 and the MSc degree in Computer Sciences from the Centre for Research and Advanced Studies, Mexico City, Mexico, in 2008. He obtained the PhD degree from the Department of Automatic Control and Systems Engineering, University of Sheffield, Sheffield, U.K., in 2014. He was previously a Research Associate at Sheffield Robotics, University of Sheffield, U.K. He is currently a Research Fellow at the Institute of Design, Robotics and Optimisation (iDRO), the School of Mechanical Engineering, University of Leeds, U.K. His research interests include haptics, touch sensing, active perception for robot control, machine learning and wearable robotics.

Tony J. Dodd received the BEng in Aerospace Systems Engineering and the PhD degree from the University of Southampton, UK. He was previously a research associate at the University of Southampton and University of Sheffield. He is currently a Professor in the Department of Automatic Control & Systems Engineering, The University of Sheffield, UK. His research interests include autonomous vehicles and robotics with particular interest on machine learning, systems engineering, control, manipulation, co-operation and swarming, mission management and optimisation.

Mat Evans received the BSc degree in Psychology, the MSc degree in Computational and Systems Neuroscience, and the PhD degree from the Department of Psychology, University of Sheffield, UK., in 2013. He was previously a research associate at the Department of Psychology and the Sheffield Centre for Robotics (SCentRo) at the University of Sheffield, Sheffield, UK. He is currently a research associate in the Neural Coding Laboratory at the University of Manchester, Manchester, UK. His research interests include computational methods for active touch sensing and robotics.

Tony J. Prescott received the M.A. degree in psychology from University of Edinburgh, Edinburgh, U.K., the M.Sc. degree in Artificial Intelligence from the University of Aberdeen, Aberdeen, U.K., and the Ph.D. degree from the Department of Psychology, University of Sheffield, Sheffield, U.K., in 1994. He is a currently a Professor of cognitive neuroscience with the Department of Psychology, University of Sheffield. He is also a Permanent Research Fellow with the Bristol Robotics Laboratory, Bristol, U.K. His research interests include the biological and brain sciences, particularly concerned with understanding the evolution, development, and function of natural intelligence and the investigation of computational neuroscience models of animal and human intelligence and in testing these models in biomimetic robots.

Nathan F. Lepora received the B.A. degree in Mathematics and the Ph.D. degree in Theoretical Physics from the University of Cambridge, U.K. He is currently a Lecturer with the Department of Engineering Mathematics, University of Bristol, U.K., and is affiliated with the Bristol Robotics Laboratory, University of Bristol and the University of the West of England, U.K. He has been program chair for the International Conference of Living Machines in 2012, 2013 and 2016. His research interests span robotics and computational neuroscience, focussing on robot and animal perception, artificial and natural decision making, and biomimetics.

1. Active tactile sensing with biomimetic and soft fingertip sensor

2. Bayesian perception for intelligent control of robot movements under the presence of uncertainty

3. Sensorimotor control strategies that improve tactile perception accuracy and speed

4. Action-perception loop for exploration of unknown object shapes using robot touch and an exploratory procedure